Malaysian Journal of Catalysis
http://mjcat.utm.my/
MJCat

Conversion of oleic acid model compound to biolubricant base oil using Al_2O_3 supported metal oxide catalyst

Y.L. Cheryl-Low, H.V. Lee*, S.B. Abd Hamid
Nanotechnology & Catalysis Research Centre (NANOCAT), Level 3, Block A, Institute of Postgraduate Studies (IPS), University of Malaya, 50603 Kuala Lumpur, Malaysia.
Corresponding author email: leehweivoon@um.edu.my

Article history :
Received 16 February 2016
Accepted 11 April 2017

GRAPHICAL ABSTRACT

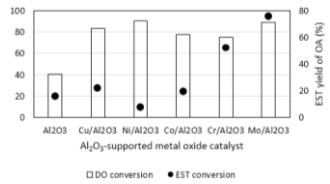

Oleic acid deoxygenation and esterification profile for Al_2O_3-supported metal oxides catalysts

ABSTRACT

Vegetable oil is commonly used as a feedstock in the lubricant industry, however recent research discovers that introduction of ester in biolubricant base oil helps enhance lubricant properties as the polar ester group is able to adhere efficiently to metal surface of lubricating system. Hence, this study focus on screening of an acid catalyst suitable for both deoxygenation and esterification for the production of hydrocarbon – ester mixture as biolubricant base oil. Alumina supported metal oxide catalysts, M/Al_2O_3 were prepared via wetness impregnation method, where M is copper (Cu), nickel (Ni), cobalt, (Co), molybdenum (Mo), and chromium (Cr). The physicochemical properties of prepared catalysts were studied via Thermo-gravimetric Analysis (TGA), X-ray Diffraction (XRD), X-ray Fluorescence Spectroscopy (XRF), Field Emission Scanning Electron Microscopy (FESEM), and Fourier Transform Infrared Spectroscopy (FTIR). XRD reveals high crystalline structure for Cu/Al_2O_3 and Mo/Al_2O_3. FESEM illustrates that Mo/Al_2O_3 has the most uniform distribution of metal oxides over alumina catalyst support. TPD-NH_3 reveals that after impregnation of Mo on Al_2O_3, there is a significant increase in acid sites of catalyst. The catalytic activity were studied via deoxygenation (5 wt. % catalyst, 3 h, 330 °C) and esterification (10 wt. % catalyst, 6 h, 70 °C and 15:1 molar ratio of methanol:oleic acid) reaction. The product selectivity and yield were determined using Gas Chromatography – Mass Spectrometry (GC-MS). The catalyst selectivity of the deoxygenated products toward n-C_{17} are arranged in the order of $Mo/Al_2O_3 > Ni/Al_2O_3 > Co/Al_2O_3 > Cr/Al_2O_3 > Cu/Al_2O_3$. As for esterification, the catalytic activity is arranged in the decreasing order of $Mo/Al_2O_3 > Cr/Al_2O_3 > Co/Al_2O_3 > Cu/Al_2O_3 > Ni/Al_2O_3$. Among the catalysts, Mo/Al_2O_3 was chosen as the potential catalyst as it rendered high deoxygenation conversion at 89 % and ester yield of 76 %.

Keywords: *Lubricant base oil; Deoxygenation; Esterification; Alumina catalyst support; Vegetable oil*

| eISSN 0128-2581 |

1. INTRODUCTION

Research has been leaning towards environment preserving awareness and focusing on converting waste biomass to renewable chemicals or energy. Automotive lubricant base oils were formerly derived from petroleum-based/ mineral oil-based, which are non-renewable and non-biodegradable. Furthermore, disposal/ leakage of lubricant gained increasing concern as large proportion of lubricant (50–60 %) disposed comes in direct contact with soil, water and air, which pose a potential threat to the ecosystem [1]. Thus, vegetable oil-based lubricant is a promising biodegradable and environmental-friendly alternative to replace the petroleum-based lubricant [2].

Generally, vegetable oil-based lubricant exhibits high viscosity index (VI) and dispersancy (convenient for mixing with additives), high flash point, high lubricity (lower friction loss, better economy of fuel), high detergency (function without detergent additives) and rapid biodegradation (reduces toxic hazard and improves waste management) as compared to conventional lubricant [3, 4]. Furthermore, vegetable oil-based lubricant has relatively low volatility due to the high molecular weight of triacylglycerol, and its lubricity is enhanced with the presence of polar ester groups, which can efficiently adhere to metal surface of the lubricating system [5]. However, the presence of ester functional group in vegetable oil-derived lubricant also causes poor stability towards oxidation and corrosion and is susceptible to hydrolysis [5], which resulted in active decomposition of fatty acid chains of lubricant, thus lowering the lubricity. Therefore, synthesis of lubricant base oil with the presence of both petrol-mimicking hydrocarbon (Fig. 1a) and ester (Fig. 1b) mixture is expected to solve the limitation of both non-biodegradable petroleum-based and unstable vegetable oil-based lubricant.

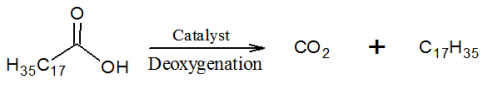

Fig. 1a Catalytic deoxygenation of oleic acid to petrol-mimicking hydrocarbon

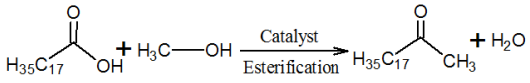

Fig. 1b Catalytic esterification of oleic acid to petrol-mimicking ester

The aim of this study is to synthesize hydrocarbon-ester based lubricant via deoxygenation and esterification of oleic acid (as a model compound of vegetable oil) by using Al_2O_3-supported metal oxide catalysts (Cu/Al_2O_3, Ni/Al_2O_3, Co/Al_2O_3, Mo/Al_2O_3, and Cr/Al_2O_3). Metal oxides supported on mesoporous support such as alumina, silica-alumina and zeolite are commonly used for the process of deoxygenation to generate biofuel. Research interest has moved from using noble metals (Pd, Pt and Ru) which are common for deoxygenation and hydrodeoxygenation reactions to the usage of inexpensive non-precious metals such as copper, nickel, cobalt, and so on. Cu, Co, Ni and Mo are commonly used as the active metal for this process [6-8]. Ni based catalyst are chosen due to their efficiency in cleaving the C-H, C-C and O-H bonds in hydrocarbons [9]. Co and Mo catalyst generally deoxygenate fatty acids via the decarbonylation pathway [10], whereas the oxygen removal pathway of Cu based catalyst is more prone to hydrodeoxygenation [11]. It was reported that Mo and Cr will result in an increase of acid sites which improves the catalytic performance for esterification [12]. Physicochemical properties of catalyst such as elemental composition, surface morphology, and chemical functional group were discussed herein. Besides, the catalytic activity for deoxygenation and esterification was investigated.

2. EXPERIMENTS

2.1 Materials

Oleic acid (OA) was purchased from R&M Chemicals. The commercial alumina catalyst support (Al_2O_3) and AR grade methanol, MeOH was purchased from Merck. The metal salts: copper(II) nitrate trihydrate, $Cu(NO_3)_2.3H_2O$, nickel(II) nitrate hexahydrate, $Ni(NO_3)_2.6H_2O$, cobalt(II) nitrate hexahydrate, $Co(NO_3)_2.6H_2O$, ammonium molybdate tetrahydrate, $(NH_3)_6Mo_7O_{24}.4H_2O$, and chromium(III) nitrate nonahydrate, $Cr(NO_3)_3.9H_2O$ were purchased from R&M Chemicals.

2.2 Synthesis of Al_2O_3-supported metal oxide catalyst

Commercial alumina (Al_2O_3) was selected as the catalyst support while the metal precursors selected for this study are $Cu(NO_3)_2.3H_2O$, $Ni(NO_3)_2.6H_2O$, $Co(NO_3)_2.6H_2O$, $(NH_3)_6Mo_7O_{24}.4H_2O$, and $Cr(NO_3)_3.9H_2O$. The samples with 10 wt. % metal loading were prepared via wetness impregnation method, where water was used as the solvent to dissolve the metal nitrate salts, which were then added dropwise to the solid alumina support and stirred continuously for 24 h at room temperature, followed by drying at 110 °C. The impregnated catalysts were calcined in air atmosphere at 500 °C for 3 h. The catalyst formed were denoted as Cu/Al_2O_3, Ni/Al_2O_3, Co/Al_2O_3, Mo/Al_2O_3 and Cr/Al_2O_3.

2.3 Catalyst characterization

Thermo-gravimetric analysis (TGA) was carried out using TGA Q500 TA Instruments to determine the thermal stability of the synthesized catalysts. X-ray Diffraction (XRD) using PANalytical Empyrean X-ray diffractometer coupled with PIXcel^{3D} detector was used to determine the chemical characteristics of the synthesized catalysts. Cu-K_α radiation of wavelengths Cu $K_{\alpha1}$ = 1.54060 Å and Cu $K_{\alpha2}$ = 1.54443 Å was employed, 2-theta range from 10° to 80° at 40 Kv and 40 mA with a step size of 0.02°. The elemental composition of the catalysts were studied via X-ray Fluorescence (XRF) analysis using PANalytical Axios X-ray Fluorescence spectrometer. The morphological studies of catalysts were carried out using Hitachi SU8030 Field Emission Scanning Electron Microscope (FESEM). Fourier Transform Infrared (FTIR) analysis was done using Perkin Elmer Fourier Transform Infrared Spectrometer to study the chemical characteristics of the catalysts. The acidity of the selected catalyst and alumina support were determined with programmed temperature (10 °C/min) from 25 °C to 900 °C by Temperature Programmed Desorption – Ammonia (TPD-NH_3) using Thermo-Finnigan TPD/R/O 1100 series apparatus equipped with thermal conductivity detector (TCD).

2.4 Catalytic deoxygenation and esterification

Catalytic deoxygenation (DO) was performed by adding 5 wt. % of synthesized catalyst into 10 g of oleic acid in a round bottom flask (Fig. 2a). The reaction was carried out at 330 °C for 3 h under partial vacuum conditions. The product was collected in a receiver flask and send for further analysis. The product yield (Equation 1) and selectivity (Equation 2) was determined using GCMS analysis whereas the DO conversion was calculated as per Equation 3 [2, 13]:

$$\text{Product Yield (\%)} = \frac{\text{Total area of product - area of reactant}}{\text{Total area of product}} \text{ x } 100\% \quad (1)$$

$$\text{Product Selectivity (\%)} = \frac{\text{Area of desired product}}{\text{Total area of product}} \text{ x } 100\% \quad (2)$$

$$\text{DO Conversion (\%)} = \frac{\text{Gas + liquid product + water}}{\text{Weight of OA}} \text{ x } 100\% \quad (3)$$

Catalytic esterification (EST) was performed by esterifying 10 g of oleic acid with 15:1 of MeOH:OA and 10 wt. % of synthesized catalyst at 70 °C for 6h under reflux conditions (Fig. 2b). The product collected was centrifuged for catalyst removal and was evaporated over 65 °C to remove unreacted MeOH. The EST yield was determined via GCMS analysis (Equation 1) whereas the EST conversion was tested via acid value (AV) test (EN 14104) and calculated as per Equation. 4 [14, 15]

$$\text{Esterification Conv. of OA (\%)} = \frac{\text{AV of OA - AV of oil sample}}{\text{AV of OA}} \text{ x } 100\% \quad (4)$$

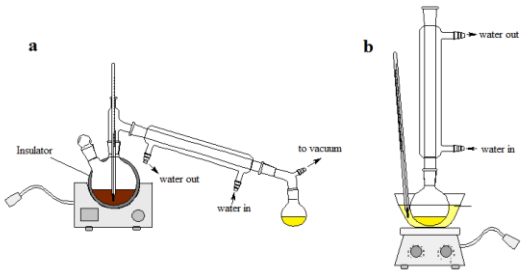

Fig. 2 Setup of (a) Deoxygenation, (b) Esterification

2.5 Qualitative characterization of product

The functional groups present in the product of deoxygenation and esterification were investigate via Fourier Transform Infrared Spectroscopy (FTIR) analysis using Perkin Elmer Fourier Transform Infrared Spectrometer, within the range from 400 – 4000 cm^{-1}. Gas Chromatography – Mass Spectrometry (GC-MS) analysis were performed using Shimadzu QP2010 equipped with non-polar column RTX-5-MS (30m x 0.25mm x 0.25µm) in split mode to identify the compounds present in the products.

3. RESULTS AND DISCUSSION

3.1 Physicochemical properties of catalysts

The thermal decomposition profile of the Al_2O_3-supported metal oxide catalysts were illustrated in Fig. 3a and 3b. It is noted that Cu/Al_2O_3 exhibits first weight loss around 170 °C due to loss of water physically bounded to the precursor's surface [16]. Similar decomposition profile was observed for Ni/Al_2O_3, where desorption of physically bound water from both precursor surface as well as hydrates from the nickel nitrates precursor at 200 °C [16, 17]. The second weight loss at temperature range of 300-350 °C was attributed to the decomposition of $Ni(NO_3)_2.6H_2O$ into stable nickel oxide. In the case of Co/Al_2O_3, $Co(NO_3)_2.6H_2O$ precursor decompose at temperature of 285 °C into Co_3O_4 oxides after experiencing water desorption at around 155 °C [18, 19]. As for Mo/Al_2O_3, the weight loss at temperature range between 300 – 450 °C is attributed by water desorption from hydrate from the molybdenum nitrate precursor [20]. Cr/Al_2O_3 losses water at 150 – 200 °C, and further losses weight at around 250 – 315 °C, due to the decomposition of nitrate compounds to nitrogen dioxide, oxygen and water, which gave rise to the formation of CrO_3 [21].

The X-ray Diffraction (XRD) patterns of Al_2O_3-supported metal oxide catalysts are illustrated in Fig. 4. All the catalysts showed the presence of Al_2O_3 phases at XRD diffraction peaks of 2θ = 37.7°, 48.7° and 67.2° (JCPDS 00-001-1308), which is similar to the XRD patterns of alumina support. Cu/Al_2O_3 catalyst rendered high crystallinity of CuO phases at diffraction peaks of 2θ = 35.6°, 38.8°, 48.8°, 61.6°, 66.3° and 68.1° (JCPDS 00-005-0661). As for Ni/Al_2O_3, two NiO peaks are identified at 2θ = 37.5° and 42.5° (JCPDS 00-047-1049). The presence of Co_3O_4 phases in Co/Al_2O_3 was exhibited at 2θ positions of 31.4°, 37.0°, 45.0°, 59.5° and 65.4° (JCPDS 00-009-0418). The major diffraction peaks of MoO_3 found in Mo/Al_2O_3 is located at 2θ = 23.4°, 25.8°, 27.4°, 33.7°, 38.8° and 49.4° (JCPDS 01-076-1003). Cr/Al_2O_3 shows its oxide phases (CrO_3) at 2θ = 33.9°, 36.5°, 45.6° and 55.2° (JCPDS 00-051-0959). The elemental composition of catalysts were determined by XRF analysis, where the metal oxide content of each catalysts: Cu/Al_2O_3, Ni/Al_2O_3, Co/Al_2O_3, Mo/Al_2O_3 and Cr/Al_2O_3 are 10.8, 12.8, 11.3, 46.6 and 12.9 atomic %, respectively. This results indicated that the metal oxide content does not deviate from intended amount (10 wt. % of metal impregnated on the Al_2O_3 support), except for Mo/Al_2O_3 catalyst. This can be explained as excess of Mo concentration will cause aggregation of Mo metal on the alumina surface hence resulted in multiple layer coatings of Mo on Al_2O_3 surface [22].

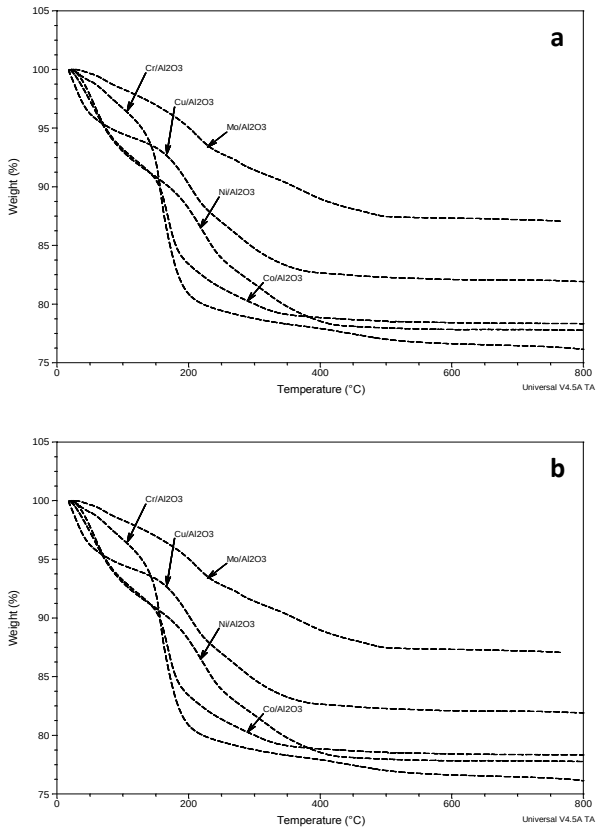

Fig. 3 Al_2O_3-supported metal oxide catalysts thermogram of (a) TGA and (b) DTG

The surface morphology of the Al_2O_3-supported metal oxide catalysts were illustrated in Fig. 5. The surface morphology of Al_2O_3 support reveals a compacted structure with flat surface. Cu/Al_2O_3 catalyst showed a surface with irregular shaped particles [23], which corresponded to CuO deposited on the surface of Al_2O_3 support [24, 25]. Similar particles structure were found in alumina supported NiO [16, 26], CoO_3 and CrO_3, where irregular aggregates were coated

on the rough surface of alumina support [25]. Interestingly, Mo/Al_2O_3 showed the presence of MoO_3 particles with spherical structure were uniformly dispersed over the surface of Al_2O_3 [27].

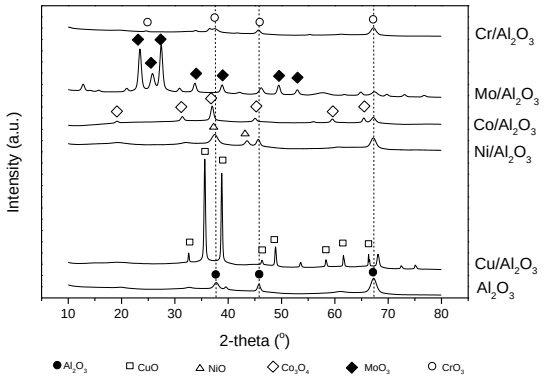

Fig. 4 XRD spectrum of Al_2O_3-supported metal oxide catalysts

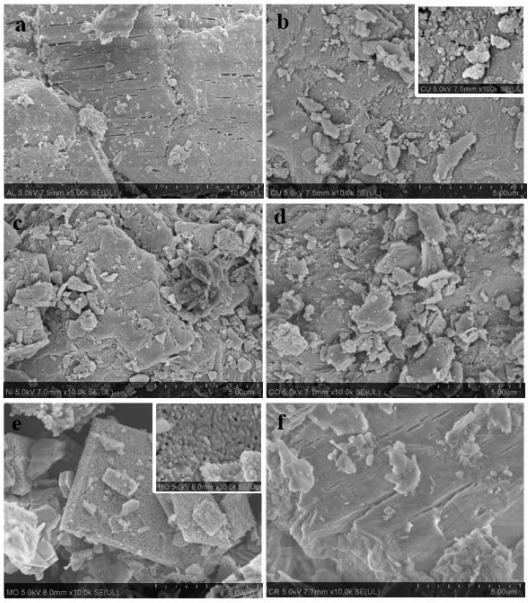

Fig. 5 FESEM micrographs of a: Al2O3, b: Cu/Al2O3, c: Ni/Al2O3, d: Co/Al2O3, e: Mo/Al2O3, and f: Cr/Al2O3

FTIR was performed to study the chemical functional groups of the Al_2O_3-supported metal oxide catalysts (Fig. 6). Al_2O_3 exhibits a small shoulder peak at 1100 cm^{-1} due to the symmetric and asymmetric of Al-O-Al bonds [28, 29]. As for Cu/Al_2O_3, the two vibration bands around 570 and 780 cm^{-1} are attributed to the Cu-O stretching [30]. It has been reported that the region between 500 – 800 cm^{-1} is assigned to M-O bands (Al-O, Cu-O, Ni-O and Co-O) [31, 32]. Mo/Al_2O_3 catalyst shows two intense peaks 880 and 985 cm^{-1}, which indicates the presence of molybdenum species and Mo−O vibrations of the octahedral species MoO_3 [28]. For all five metal oxide catalyst supported on Al_2O_3, they exhibits three vibrational frequencies at similar position, where the 2370 cm^{-1} is assigned to the asymmetric vibration of CO_2 from atmospheric carbon dioxide [16], while 1655 and 3450 cm^{-1} are attributed by the hydroxide (O-H) functional group from the absorbed water after calcination [16, 29, 33].

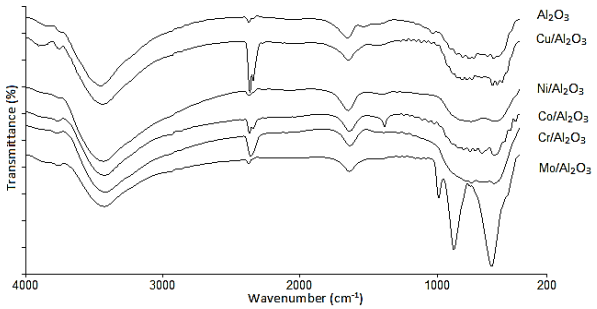

Fig. 6 FTIR spectrum of Al2O3-supported metal oxide catalysts

The acidity of Al_2O_3 and Mo/Al_2O_3 was determined by TPD-NH_3. Fig. 7 shows that Al_2O_3 has low amount of acidity (892.07 µmol/g). The two peaks present in Fig. 7 for alumina showed that both active sites rendered weak and medium acid strength [34]. Mo/Al_2O_3 however, proved that the incorporation of Mo into alumina has led to an increase in acidity [35, 36] (3582.79 µmol/g) where majority of the acidic sites were weak [34]. Molybdenum has been reported to be an effective promoter that enhance surface acidity by increasing active sites of the catalyst. It is known that MoO_3 increases Brønsted acidity which led to generation of acid active sites on surface of catalyst, hence resulting in higher acidity in Mo/Al_2O_3 [22].

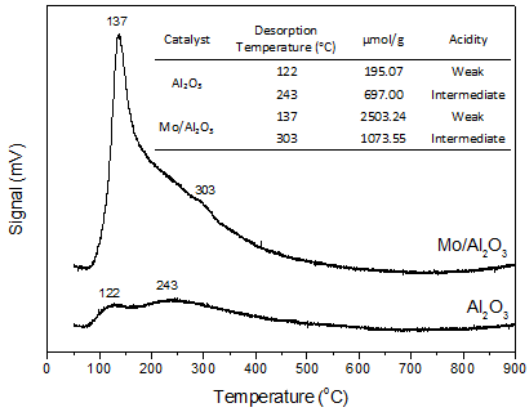

Catalyst	Desorption Temperature (°C)	µmol/g	Acidity
Al_2O_3	122	195.07	Weak
	243	697.00	Intermediate
Mo/Al_2O_3	137	2503.24	Weak
	303	1073.55	Intermediate

Fig. 2 TPD-NH_3 profile of Al_2O_3 and Mo/Al_2O_3

3.2. Catalytic deoxygenation and esterification

3.2.1 Quantitative analysis of products

Catalytic deoxygenation and esterification of oleic acid was performed by using different types of Al_2O_3-supported metal oxide catalysts (Table 1 and Fig. 8). For comparison purposes, catalytic activity of blank Al_2O_3 without impregnation with other metals was also tested via deoxygenation and esterification reaction. For

deoxygenation, blank alumina gave the highest DO conversion (81.1 %), however, most of the products were mainly the products of cracking (C_5 - C_{15}). With impregnation of other metal, the selectivity shifts towards C_{17} hydrocarbon. For esterification reaction, blank alumina gave second lowest ester yield (15.8 %) after Ni/Al_2O_3. After incorporation of metals, based on the deoxygenation profile, Ni/Al_2O_3 showed the highest oleic acid conversion (91 %) followed by Mo/Al_2O_3 (89 %) and Cu/Al_2O_3 (83 %). For esterification reaction however, Ni/Al_2O_3 gave the lowest ester yield (7 %) while Cr/Al_2O_3 and Mo/Al_2O_3 yield 52% and 76% respectively. The low yield of ester was due to low acidic characteristics of the catalyst, where most of the acidity was contributed by alumina support [37]. However, after impregnated with molybdenum, as shown in TPD-NH_3 analysis, the acidity of catalyst is significantly improved as MoO_3 aids to increase the amount of strong acidic sites to the catalyst [35]. Catalyst with high acidity is required to perform well in esterification, however, if the acidity is too strong, it will not be suitable for deoxygenation process as it will favour cracking to shorter chain products. Hence, Mo/Al_2O_3 is suitable for both deoxygenation and esterification as the acid sites are increased significantly but most of the acid sites are of weak and medium acidic strength.

Table 1 Oleic acid conversion and product yield for deoxygenation and esterification reaction

Catalyst	DO conversion (%) [a]	Yield of HC (%) [b]	EST conversion (%) [c]	EST yield (%) [b]
Al_2O_3	40.1	81.1	9.2	15.8
Cu/Al_2O_3	83.3	31.6	10.4	21.6
Ni/Al_2O_3	90.7	29.7	8.9	7.4
Co/Al_2O_3	77.6	17.6	11.7	19.0
Cr/Al_2O_3	75.1	28.8	15.3	52.0
Mo/Al_2O_3	89.0	30.8	31.1	75.8

a: Calculated by using Equation 3
b: Calculated by peak area % by GC-MS using Equation 1
c: Calculated by using Equation 4

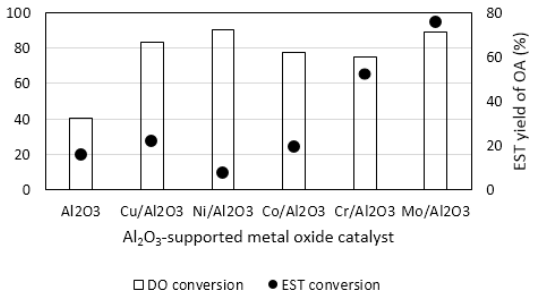

Fig. 83 Oleic acid deoxygenation and esterification profile for Al_2O_3-supported metal oxides catalysts

Table 2 Effect of catalyst on product selectivity

Catalyst	Product Selectivity (Peak Area, %)					
	$C_6 - C_{15}$	C_{16}	C_{17}^a	C_{17}^b	C_{17}^c	C_{18}
Al_2O_3	68.9	3.2	10.8	2.1	-	15.1
Cu/Al_2O_3	29.3	58.0	7.1	2.0	2.8	0.8
Ni/Al_2O_3	17.9	42.8	33.8	3.4	1.6	0.6
Co/Al_2O_3	32.0	8.1	14.4	3.5	-	42.0
Cr/Al_2O_3	36.7	7.8	11.3	2.4	-	41.7
Mo/Al_2O_3	13.2	1.9	53.8	4.7	2.6	23.7

C_{17}^a: C_{17} alkene, heptadecene
C_{17}^b: C_{17} alkane, heptadecane
C_{17}^c: C_{17} compounds besides alkane and alkene, such as alcohols, alkynes and aldehydes

3.2.2 Qualitative analysis of products

The selectivity of Al_2O_3-supported metal oxide catalyst toward deoxygenation were analyzed via GC-MS, by calculating the percentage of n-alkene and n-alkane produced (Equation 2) [38].

By observing the yield of C_{17}-alkene and alkane in Table 2, it can be concluded that all five Al_2O_3-supported metal oxide catalyst shows greater degree of selectivity toward decarbonylation (the removal of one molecule of carbon monoxide and one molecule of water to form an unsaturated hydrocarbon chain) as compared to decarboxylation (the removal of a molecule of carbon dioxide to yield a saturated hydrocarbon chain) [39, 40]. The reaction of decarboxylation and decarbonylation are illustrated in Equation 4 and 5 [41, 42].

Decarboxylation:

$$RCOOH \longrightarrow RH + CO_2 \quad (4)$$

Decarbonylation:

$$RCOOH + H_2 \longrightarrow R'H + CO + H_2O \quad (5)$$

Hydrodeoxygenation:

$$RCOOH + 3H_2 \longrightarrow R'H + 2H_2O \quad (6)$$

R = saturated alkyl group
R' = unsaturated alkyl group

The results revealed that besides decarboxylation and decarbonylation, hydrogenation and hydrodeoxygenation (Equation 6) also exist. This is proven by the presence of

compounds with even number of carbon atoms in the product [43]. Among the catalyst, Co/Al_2O_3 and Cr/Al_2O_3, are found to show lower selectivity toward decarboxylation/ decarbonylation, but has a greater degree of hydrodeoxygenation side reaction. This is proven by the high percentage of a C_{18} alcohol, 9-octadecen-1-ol, $C_{18}H_{36}O$ present in the deoxygenated product (Table 1). This alcohol is formed as a result of a side reaction of hydrodeoxygenation of oleic acid, $C_{18}H_{34}O_2$. Mo/Al_2O_3 however, although shown significant amount of 9-octadecen-1-ol (23.7 %), it has greater selectivity toward decarbonylation (53.8 %). Cu/Al_2O_3 and Ni/Al_2O_3 also show significant selectivity toward the side reaction of hydrodeoxygenation (58.0 % and 42.8 % yield of 9-hexadecen-1-ol respectively), but only after oleic acid was cracked to C_{16}. This phenomenon may be due to after decarboxylation, decarbonylation and cracking, the carbon monoxide (result from decarbonylation of the ester group, -COO) and methane (result from cracking of the fatty acid chain) formed undergo reaction with the water produced as a by-product. This reaction is known as steam reforming, where methane reacts with steam under low temperature (300 °C) [44] over a metal oxide, and hydrogen is generated in-situ for this reaction. The hydrogen aids the hydrodeoxygenation process of C_{16} hydrocarbon and converts it to 9-hexadecen-1-ol. Based on the result of GC-MS, an assumption can be made that in the presence of hydrogen, Cu/Al_2O_3 will give the highest degree of hydrodeoxygenation. The selectivity of the deoxygenated products toward n-C_{17} are arranged in the order of Mo/Al_2O_3 > Ni/Al_2O_3 > Co/Al_2O_3 > Cr/Al_2O_3 > Cu/Al_2O_3, whereas the hydrodeoxygenation selectivity are of the reversed order.

The functional groups of the reactant, oleic acid, as well the products from deoxygenation by different type of catalysts were analyzed via FTIR spectroscopy. Whereas, only the product from esterification catalyzed by Mo/Al_2O_3 catalyst was analyzed as the rest of the catalysts failed to produce significant amount of ester. Fig. 9 shows the presence of two intense peaks for all DO products as well as oleic acid at 2923 and 2854 cm^{-1}, indicates the asymmetric and symmetric vibrations of methylene group (CH_2) respectively [45, 46]. The weak adsorption band at 3007 cm^{-1} is attributed to =C-H stretching of the carbon-carbon double bonds [45, 47-49]. The existence of peak at 1708 cm^{-1} indicates the presence of carbonyl group (C=O) [48] from oleic acid, showing that the product is not fully deoxygenated as the reactant is still present in them [45]. The symmetric vibration modes of –COOH were shown at 1460 cm^{-1} with medium intensity [45, 50]. A weak intensity peak at 1376 cm^{-1} is assigned to terminal methyl group (CH_3) [51]. Fig. 10 compares the ester product of Mo/Al_2O_3 with oleic acid, its reactant. The presence of ester is confirmed by the adsorption bands of C=O (1744 cm^{-1}) and C-O stretch (1247 and 1171 cm^{-1}) from ester group [52, 53]. However, the adsorption of C=O carbonyl group from oleic acid is also found present in the ester product, which means the esterification reaction is not complete. The disappearance of O-H bend from carboxylic acid at 936 cm^{-1} also indicates the conversion of oleic acid to ester [52].

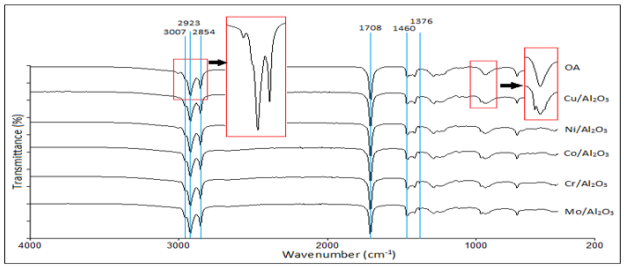

Fig. 9 FTIR spectrum of deoxygenation product catalyzed by Al_2O_3-supported metal oxide catalysts

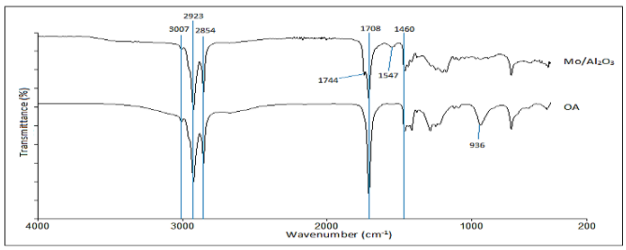

Fig. 10 FTIR spectrum of esterification product catalyzed by Al_2O_3-supported metal oxide catalysts

4. CONCLUSION

A metal oxide supported catalyst, suitable to catalyst both deoxygenation and esterification was successfully synthesized for the production of hydrocarbon-ester mixture for lube base oil application. XRD reveals high crystalline structure for Cu/Al_2O_3 and Mo/Al_2O_3. FESEM illustrates that Mo/Al_2O_3 has the most uniform distribution of metal oxides over alumina catalyst support. TPD-NH_3 reveals that after impregnation of Mo on Al_2O_3, there is a significant increase in acid sites of catalyst. The catalyst performance on selectivity of deoxygenated products toward n-C_{17} are arranged in the order of Mo/Al_2O_3 > Ni/Al_2O_3 > Co/Al_2O_3 > Cr/Al_2O_3 > Cu/Al_2O_3 with yield in the range of 7 – 54 %. As for esterification, the catalytic activity is arranged in the decreasing order of Mo/Al_2O_3 > Cr/Al_2O_3 > Co/Al_2O_3 > Cu/Al_2O_3 > Ni/Al_2O_3 in the range of 7 – 76 % yield. Among the catalysts synthesized for deoxygenation and esterification of oleic acid, Ni/Al_2O_3 and Mo/Al_2O_3 shows potential characteristics for further studies in improving the production of biolubricant in the presence of hydrogen gas. Ni/Al_2O_3 demonstrates the highest performance on deoxygenation reaction (90.7 %) followed by Mo/Al_2O_3 (89.0 %). Mo/Al_2O_3 was chosen as the potential catalyst as it rendered high deoxygenation conversion at 89.0 % and ester yield of 75.8 %. In future studies, the combination of these two metals may lead to improvement of the OA conversions. Deoxygenation in the presence of hydrogen is also expected to improve the lubricity of biolubricant, higher thermal-oxidative stability (elimination of formation of alkenes) and at the same time lower the reaction conditions

required, such as reaction temperature, time and catalyst loading.

ACKNOWLEDGEMENTS

Financial support from University of Malaya's Grand Challenge grant (GC, Project number: GC001B-14AET), and Postgraduate Research Grant (PPP, Project number: PG061-2015A).

NOMENCLATURE

DO : Deoxygenation
DTG : Thermogravimetric derivative
EST : Esterification
FESEM : Field Emission Scanning Electron Microscopy
GC-MS : Gas Chromatography – Mass Spectrometry
MeOH : Methanol
OA : Oleic acid
TGA : Thermogravimetric analysis
TPD-NH_3 : Temperature Programmed Desorption - Ammonia
XRD : X-ray Diffraction
XRF : X-ray Florescence Spectrometry

REFERENCES

[1] P. Nagendramma, S. Kaul, Renew. Sustainable Energy Rev. 16(1) (2012) 764.
[2] S. El Khatib, S. Hanafi, M. Arief, E. Al-Amrousi, Petrol. Sci. Technol. 5(2) (2015) 59.
[3] J. Salimon, N. Salih, E. Yousif, Eur. J. Lipid Sci. Tech. 112(5) (2010) 519.
[4] H.M. Mobarak, E.N. Mohamad, H.H. Masjuki, M.A. Kalam, K.A.H. Al Mahmud, M. Habibullah, A.M. Ashraful, Renew. Sustainable Energy Rev. 33 (2014) 34.
[5] C.S. Madankar, A.K.Dalai, S.N. Naik, Ind. Crop. Prod. 44 (2013) 139.
[6] R. Loe, E. Santillan-Jiminez, T. Morgan, L. Sewell, Y. Ji, S. Jones, M. A. Isaacs, A. F. Lee, M. Crocker, Appl. Catal., B 191 (2016) 147.
[7] V. Han-u-domlarpyos, P. Kuchonthara, P. Reubroycharoen, N. Hinchiranan, Fuel 143 (2015) 512.
[8] N. Asikin-Mijan, H. V. Lee, G. Aldulkareem-Alsultan, A. Afandi, Y. H. Taufiq-Yap, J. Clean. Prod (2016) 1.
[9] G. Sadanandam, K. Ramya, D. B. Kishore, V. Dugakumari, M. SubrahmanyamK. V. R. Chary, RSC Adv. 4(6) (2014) 32429.
[10] G. J. S. Dawes, E. L. Scott, J. Le Notre, J. P. M. Sanders, J. H. Bitter, Green Chem. 17(6) (2015) 3231.
[11] K. A. Rogers, Y. Zheng, ChemSusChem 9(14) (2016) 1750.
[12] X. Li, H. Cheng, G. Liang, L. He, W. Lin, Y. Yu, F. Zhao, Catalysts 5(2) (2015) 759.
[13] Y.S. Ooi, R. Zakaria, A.R. Mohamed, S. Bhatia, Biomass Bioenerg. 27(5) (2004) 477.
[14] J. Xu, J. Zhang, X. Yin, D. Yang, H. Zhang, J. Qian, L. Liu, X. Liu, Braz. J. Chem. Eng. 28 (2011) 259.
[15] Y.L. Cheryl-Low, K.L. Theam, H.V. Lee, Energ. Convers. Manage. 106 (2015) 932.
[16] S.M. Sajjadi, M. Haghighi, A.A. Eslami, F. Rahmani, J. Sol-Gel Sci. Techn. 67(3) (2013) 601.
[17] N. Rahemi, M. Haghighi, A.A. Babaluo, M.F. Jafari, S. Khorram, Int. J. Hydrogen Energ. 38(36) (2013) 16048.
[18] L. Ji, J. Lin, H. Zeng, J. Phys. Chem. B 104(8) (2000) 1783.
[19] W. Chu, P.A. Chernavskii, L. Gengembre, G.A. Pankina, G.A. Pankina, P. Fongarland, A.Y. Khodakov, J. Catal. 252(2) (2007) 215.
[20] Y. Cui, N. Liu, Y. Xia, J. Lv, S. Zheng, N. Xue, L. Peng, X. Guo, W.Ding, J. Mol. Catal. A Chem. 394 (2014) 1.
[21] W.Z. Lang, C.L. Hu, L.F. Chu, Y.J Guo, RSC Adv. 4(70) (2014) 37107.
[22] J. Deng, J. Liu, W. Song, Z. Zhao, L. Zhao, H. Zheng, A. C. Lee, Y. Chen, J. Liu, RSC Adv. 7(12) (2017) 7130.
[23] M.I. Dar, S. Sampath, S.A Shivashankar, J. Mater. Chem. 22(42) (2012) 22418.
[24] N. Mukherjee, S. Ahammed, S. Bhadra, B.C. Ranu, Green Chem., 15(2) (2013) 389.
[25] S.M. Pudi, P. Biswas, S. Kumar, B. Sarkar, J. Brazil. Chem. Soc. 26 (2015) 1551.
[26] Y. Du, R. Chen, Chem. Biochem. Eng. Q., 21(3) (2007) 251.
[27] J. SongáChen, X. WenáLou, Chem. Commun. 46(37) 2010) 6906.
[28] S. Badoga, R.V. Sharma, A.K. Dalai, J. Adjaye, Ind. Eng. Chem. Res. 53(49) (2014) 18729.
[29] J. Ryczkowski, Catal. Today, 68(4) (2001) 263.
[30] P. Estifaee, M. Haghighi, N. Mohammad, F. Rahmani, Ultrason. Sonochem. 21(3) (2014) 1155.
[31] M. Sharifi, M. Haghighi, F. Rahmani, S. Karimipour, J. Nat. Gas Sci. Eng. 21 (2014) 993.
[32] S.R. Yahyavi, M. Haghighi, S. Shafiei, M. Abdollahifar, F. Rahmani, Energ. Convers. Manage. 97 (2015) 273.
[33] N. Rahemi, M. Haghighi, A.A. Babaluo, M.F, Jafari, S. Allahyari, Korean J. Chem. Eng. 31(9) (2014) 1553.
[34] A. Ramli, M. Farooq, MJAS, 19(1) (2015) 8.
[35] K.V.R Chary, K. Reddy, Rajender, G. Kishan, J.W. Niemantsverdriet, G. Mestl, J. Catal. 226(2) (2004) 283.
[36] G. Mitran, O. Pavel, React. Kinet. Mech. Cat. 114(1) (2015) 197.
[37] O.S. Joo, K.D. Jung, S.H. Han, B. Kor. Chem. Soc. 23(8) (2002) 1103.
[38] N. Asikin-Mijan, H.V Lee., Y.H. Taufiq-Yap, J.C. Juan, N.A. Rahman, J. Anal. Appl. Pyrol. 117 (2016) 46.
[39] J.G. Immer, M.J. Kelly, and H.H. Lamb, Appl. Catal. A-Gen. 375(1) (2010) 34.
[40] J.P. Ford, J.G. Immer, H.H. Lamb, Top. Catal. 55(3-4) (2012) 175.
[41] L. Hermida, A.Z. Abdullah, A.R Mohamed., Renew. Sust. Energ. Rev. 42 (2015) 1223.
[42] S. Lestari, P. Mäki-Arvela, J. Beltramini, G.Q.M. Lu, D.Y. Murzin, ChemSusChem 2(12) (2009) 1109.
[43] Ł. Jęczmionek, K. Porzycka-Semczuk, Fuel 128 (2014) 296.
[44] F. Mariño, M. Boveri, G. Baronetti, M. Laborde, Int. J. Hydrogen Energ. 26(7) (2001) 665.
[45] Y. Ding, X. Zhang, H. Zhu, J. Zhu, J. Mater. Chem. C 2(5) (2014) 946.
[46] G. Marcelo, A. Munoz-Bonilla, J. Rodriguez-Hernandez, M. Fernandez-Garcia, Polym. Chem. 4(3) (2013) 558.
[47] N.A. Gomez, R. Abonia, H. Cadavid, I.H. Vargas, J. Brazil. Chem. Soc. 22(12) (2011) 2292.
[48] C.M.P. de Souza, D.P.G. dos Santos, C.P. de Santana, D.P. Santana, Afr. J. Pharm. Pharmacol. 8(33) (2014) 824.
[49] M.L.S. Albuquerque, I. Guedes, J.P. Alcantara, S.G.C. Moreira, Vib. Spectrosc. 33(1–2) (2003) 127.
[50] K.L. Lei, C.F. Chow, K.C. Tsang, E.N.Y. Lei, V.A.L. Roy, M.H.W. Lam, C.S. Lee, E.Y.B. Pun, J. Li, J. Mater. Chem. 20(35) (2010) 7526.
[51] A.M. Gumel, M.S.M. Annuar, T. Heidelberg, PLoS ONE 7(9) (2012) e45214.
[52] M. Tariq, S. Ali, F. Ahmad, M. Ahmad, M. Zafar, N. Khalid, M.A. Khan, Fuel Process. Technol. 92(3) (2011) 336.
[53] I.P. Soares, T.F. Rezende, R.C. Silva, E.V.R. Castro, R. Vinicius, I.C.P. Fortes, Energ. Fuel. 22(3) (2008) 2079.